

NASA CR-1044

**RADIATIVE HEATING AND COOLING FUNCTIONS FOR THE LOWER  
MARTIAN ATMOSPHERE UNDER THE CONDITION OF  
LOCAL THERMODYNAMIC EQUILIBRIUM (LTE)**

By Albert J. Pallmann

Distribution of this report is provided in the interest of information exchange. Responsibility for the contents resides in the author or organization that prepared it.

Issued by Originator as Report No. 101

Prepared under Grant No. NGR 26-006-016 by  
SAINT LOUIS UNIVERSITY  
St. Louis, Mo.

for Langley Research Center

NATIONAL AERONAUTICS AND SPACE ADMINISTRATION

---

For sale by the Clearinghouse for Federal Scientific and Technical Information  
Springfield, Virginia 22151 - CFSTI price \$3.00

## Abstract

The physics of planetary radiation fields has been re-examined to derive formulae describing analytically the heating and cooling processes of the Martian atmosphere in local thermodynamic equilibrium (LTE). The computational algorithm required for the numerical solution of the radiative heating and cooling in the Martian atmosphere has been outlined. Spectral data for near and far IR CO<sub>2</sub> bands have been provided.

A model was assumed for the Martian atmosphere in LTE, characterized by 100% CO<sub>2</sub>, plane-parallel stratification, with no particulates embedded, scattering by molecules excluded, and neglecting the reflection of solar radiation at the ground. However, radiative equilibrium has not been assumed, because this assumption would have made the heating and cooling rates identically zero. Since mechanisms other than radiation are assumed to transport heat in the atmosphere, the condition of radiative equilibrium would be senseless.

A quasi-random model has been used to arrive at an appropriate analytic form of the transmission function. This function is then inserted in the mathematical expressions of the integrated upward and downward fluxes at the parametric reference level. The downward flux formula includes solar radiation and atmospheric long-wave radiation, whereas the upward flux expression involves the Martian surface and atmospheric layer radiation.

The numerical values of CO<sub>2</sub> transmission in the spectral region from 1 - 20 micron have been calculated by Stull, Wyatt and Plass. The appropriate band parameters were obtained from Prabhakara and Hogan's investigation.

The radiative transfer theory, its computational algorithm, and the spectral data of CO<sub>2</sub> and solar radiation for the Martian atmosphere, as presented in this paper, provide the means for computing the radiative heating and cooling rates for the atmosphere of Mars at any latitude, once the temperature sounding is given for the location.

PRECEDING PAGE BLANK NOT FILMED.

### Acknowledgment

The author gratefully acknowledges the support of the research, presented in this report, by the National Aeronautics and Space Administration under the grant NGR-26-006-016, together with the prior assistance of the McDonnell-Douglas Corporation, St. Louis, Missouri.

## TABLE OF CONTENTS

|   |     |
|---|-----|
| Acknowledgments.....  | iii |
| Table of Contents.....  | v   |
| Table of Illustrations.....   | vi  |
| Table of Symbols.....   | vii |
| I. Introduction   |     |
| 1 - The <u>model</u> atmosphere of Mars.....  | 1   |
| 2 - The heating and cooling rate.....   | 2   |
| II. The derivation of the heating and cooling rate  |     |
| 1 - Schwarzschild's equation of radiative transfer.....   | 4   |
| 2 - Kirchhoff's law.....  | 6   |
| 3 - Local Thermodynamic Equilibrium (LTE).....  | 6   |
| 4 - The integral of the Schwarzschild equation with<br>respect to the depth $x$ .....   | 7   |
| 5 - The integral of the Schwarzschild equation with<br>respect to zenith and azimuth angles: <u>the spectral</u><br>flux..... | 11  |
| 6 - The integral with respect to the frequency: the<br><u>total flux</u> .....  | 14  |
| 7 - The transmission function.....  | 14  |
| 8 - Direct absorption of solar radiation by $\text{CO}_2$ .....   | 19  |
| III. The computational procedure  |     |
| 1 - The analytical expression of the heating and cooling<br>rate.....   | 23  |
| 2 - The computational form of the fluxes.....   | 24  |
| 3 - The computation of the heating or cooling rate.....   | 31  |
| IV. Appendices  |     |
| 1 - Appendix I: Table of the $\text{CO}_2$ band parameters.....   | 34  |
| 2 - Appendix II: Solar spectral irradiance data.....  | 38  |
| 3 - Bibliography.....   | 40  |

List of Illustrations

| <u>Figure</u>   | <u>Page</u> |
|---|-------------|
| 1. Basic geometry underlying the equation of radiative transfer for the downward intensity of a planetary atmosphere..... | 5.          |
| 2. Qualitative presentation of the CO <sub>2</sub> band absorption in the lower Martian atmosphere.....                   | 10.         |
| 3. Basic geometry underlying the equation of radiative transfer for the upward intensity of a planetary atmosphere..      | 12.         |
| 4. Geometry relating latitude, $\phi$ , to the effective projection...  | 21.         |
| 5a. Basic geometry for calculation of flux transmissivity.....  | 29.         |
| 5b. An example of $\mathcal{T}$ at reference level $x_0$ .....  | 29.         |
| 6. Outlay of computational scheme.....  | 33.         |

## List of Symbols

|                   |  |
|-------------------|--|
| $B_\nu$           | specific intensity of black body radiation                   |
| $c$               | speed of light   |
| $d$               | line spacing   |
| $E_o^s$           | solar energy within the frequency interval $(\nu, \nu+d\nu)$ |
| $E_\nu$           | spectral radiant energy                                      |
| $\underline{F}$   | total heat flux  |
| $\underline{F}_a$ | advective heat flux  |
| $\underline{F}_m$ | molecular heat flux  |
| $\underline{F}_r$ | radiative heat flux  |
| $\underline{F}_t$ | turbulent heat flux  |
| $F_{\nu,b}$       | spectral net flux for black body radiation                   |
| $h$               | heating or cooling rate, or Planck's constant                |
| $I_\nu$           | spectral specific intensity of radiation                     |
| $\mathcal{J}_\nu$ | source function  |
| $j_\nu$           | spectral emission coefficient                                |
| $K$               | Boltzmann's constant   |
| $m$               | mass   |
| $n$               | wave number  |
| $p$               | pressure   |
| $S$               | integrated line intensity                                    |
| $T$               | temperature  |
| $t$               | time   |
| $w$               | radiational path length                                      |
| $X$               | geometric depth  |

List of Symbols cont.

|                 |   |
|-----------------|---|
| $\alpha$        | line half-width   |
| $\Gamma$        | coefficient of temperature dependence of the line intensity                   |
| $\theta$        | zenith angle  |
| $\kappa_\nu$    | mass absorption coefficient for radiation in spectral range $(\nu, \nu+d\nu)$ |
| $\mu$           | $\cos \theta$   |
| $\mu_\nu$       | index of refraction (function of frequency $\nu$ )                            |
| $\nu$           | frequency   |
| $\rho$          | (mass) density  |
| $\rho(x)$       | density of radiatively active matter as function of depth $x$                 |
| $\mathcal{T}$   | transmission function   |
| $\mathcal{T}_F$ | flux transmissivity   |
| $\tau$          | optical depth   |
| $\phi$          | azimuth, or latitude  |
| $\omega$        | solid angle   |

## I. Introduction

1 - The adopted model of the Martian atmosphere.

In order to formulate analytically the circulation of the Martian atmosphere, the radiative processes must be considered. The physical need for this consideration may be seen in the way an atmospheric system receives and converts radiant energy, i. e., absorbing solar radiation and truly emitting long-wave radiation by means of an intrinsic transfer mechanism. Because of the complexity of the interaction between various layers of the Martian atmosphere and the radiation quanta of numerous frequencies and different directions, it is advisable to define an atmospheric model. The one adopted here is described by means of the following conditions:

- 1) the atmosphere is planetary and finite consisting of 100% CO<sub>2</sub>; no other constituent considered;
- 2) no suspensoids in this model atmosphere; model "air" is clean;
- 3) no scattering present (for clean "air" it would be a Rayleigh type of scattering);
- 4) local thermodynamic equilibrium (LTE) existent up to 50 km.;
- 5) Doppler broadening of the spectral lines negligible (this assumption appears to be less critical than the one of LTE); Doppler broadening might become important beyond 80 km. in the Martian atmosphere;
- 6) the surface of Mars as the lower boundary of its atmosphere is assumed not to reflect any solar radiation, although the ground is represented by an infinitely large optical depth with respect



to IR radiation; the latter assumption is applied to terrestrial conditions.

At this point, it is proposed to plan further study in this sector in such a way that the set of assumptions is gradually diminished. Modifications of the rather restricted model should be expected, if other constituents are permitted or scattering is included, to give but two examples. Since the computations of the heating and cooling rates will be carried out from the ground level up to 50 km., no photochemical processes will be discussed in this report. Those processes become increasingly important beyond 65 km., where the molecules and atoms emit and absorb at a rate which is determined by the incident radiation rather than by their temperature.

## 2 - The heating and cooling rate.

As known from the terrestrial atmosphere, there is a very essential connection between radiative transfer and atmospheric fluid motion. If one wants to obtain deeper insight into the nature of atmospheric motions, specially those created in the convective troposphere, one must investigate the distribution of the radiative fluxes and their connection with advective, turbulent and molecular heat fluxes.

The heating or cooling rate in an atmospheric fluid system is given by Goody (1964) as:

$$(1) \quad h = -\nabla \cdot \underline{F} = -\nabla \cdot (\underline{F}_r + \underline{F}_a + \underline{F}_t + \underline{F}_m).$$

where

$\underline{F}$  : total heat flux

$\underline{F}_t$  : turbulent heat flux

$\underline{F}_r$  : radiative heat flux

$\underline{F}_m$  : molecular heat flux

$\underline{F}_a$  : advective heat flux

$$h = \rho c_p \frac{\partial T(x, y, z, t)}{\partial t}$$

The concept "flux" used here actually means net flux. Thus, it is realized that the radiative net fluxes should be considered in order to obtain the radiative heating or cooling rates. These are given, as the above formula shows, by means of the divergence of the radiative heat flux. Since the assumption is generally made that a planetary atmosphere consists of plane-parallel layers of homogeneous and isotropic distribution of matter, only the vertical divergence needs to be taken into account. The computational details will be discussed in section III.

## II. The derivation of the heating and cooling rates.

### 1 - Schwarzschild's equation of radiative transfer.

A critical review of the basic radiative transfer formulae and their derivations is appropriate. The procedure chosen is related to the analytical development Kourganoff (1963) has presented.

The equation of radiative transfer according to Schwarzschild (1906) is given by:

$$(2) \quad \frac{\mu}{\rho(x) \cdot \kappa_{\nu}(x, \nu)} \frac{d}{dx} I_{\nu}(x, \mu, \nu) = I_{\nu}(x, \mu, \nu) - \mathcal{J}_{\nu}(x, \nu)$$

which is the analytical form referring to

- 1) a plane parallel atmosphere
- and 2) radiation within the spectral interval  $(\nu, \nu+d\nu)$ .

The symbols have the following meaning:

$\mu = \cos\theta$  : with  $\theta$ : zenith angle

$\rho(x)$  : density of the radiatively active matter as a function of the depth  $x$

$\kappa_{\nu}(x, \nu)$  : mass absorption coefficient for radiation within the spectral range  $(\nu, \nu+d\nu)$ .

$I_{\nu}$  : spectral specific intensity of radiation

$\mathcal{J}_{\nu}$  : source function

The underlying geometry is indicated by Figure 1.

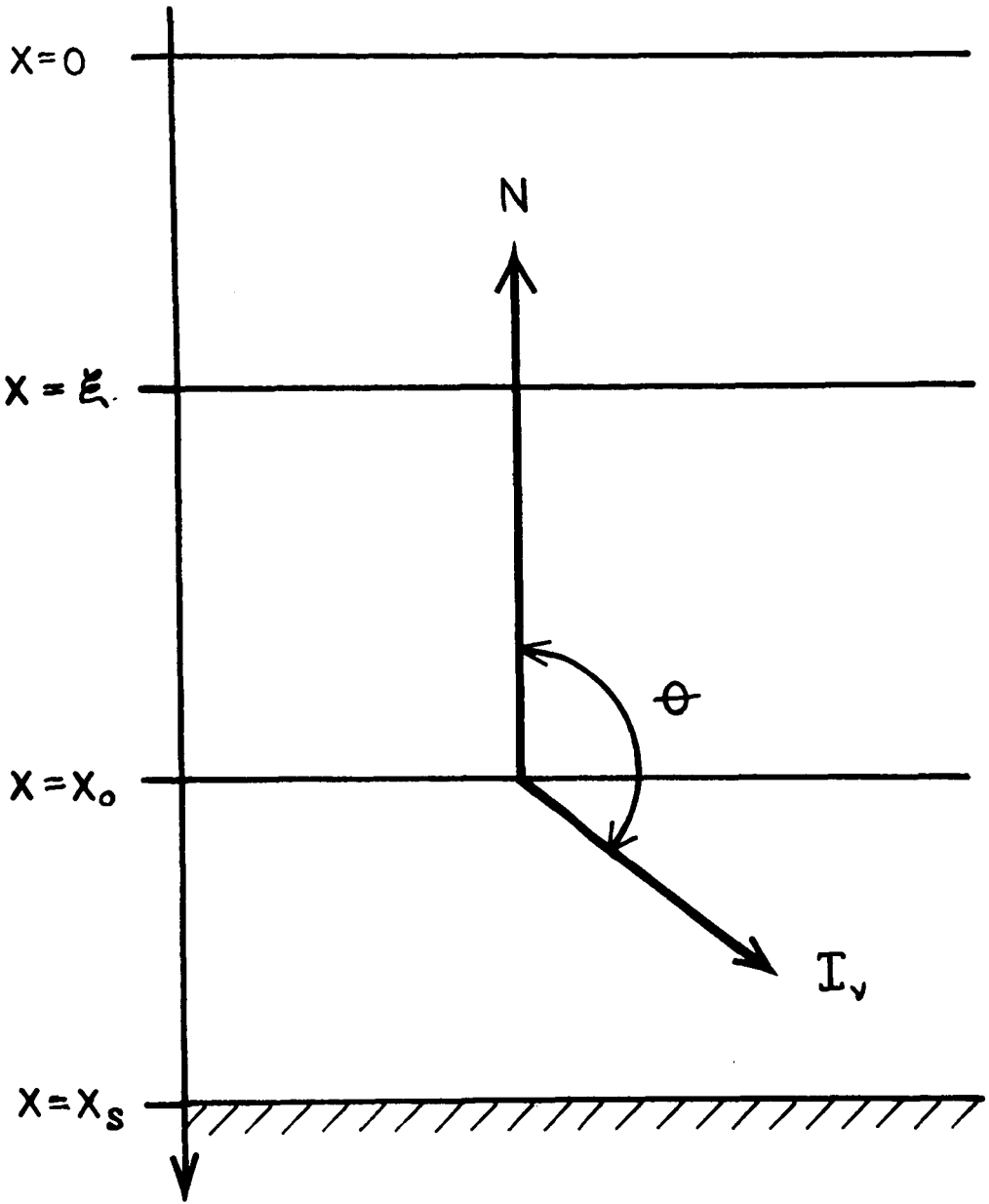


FIG 1

## 2 - Kirchhoff's law.

The assumption is made that Kirchhoff's law is valid:

$$(3) \quad j_{\nu} = \mu_{\nu}^2 \kappa_{\nu} \cdot B_{\nu}(T)$$

where  $j_{\nu}$  is the spectral emission coefficient defined by:

$$(4) \quad j_{\nu} = \frac{dE_{\nu}}{d\nu d\omega dt dm}$$

with

$dE_{\nu}$ : differential of the spectral energy

$d\omega$ : elementary solid angle (steradian)

$dm$ : elementary mass

$\mu_{\nu}$ : index of refraction (function of frequency  $\nu$ )

$\kappa_{\nu}$ : spectral absorption coefficient defined by  $dI_{\nu} = -I_{\nu} \kappa_{\nu} \rho ds$

$B_{\nu}$ : spectral specific intensity of black radiation (or better enclosure radiation).

It follows from the validity of Kirchhoff's law that molecular collisions are of sufficient importance as a cause of molecular absorptions and emissions. Collision battering happens at a large enough rate, so that the molecules assume a state characteristic of thermodynamic equilibrium at the temperature  $T$ .

## 3 - Local Thermodynamic Equilibrium (LTE)

The concept of Local Thermodynamic Equilibrium was defined by Schwarzschild (1906). It is intimately connected with Kirchhoff's law. The circumstance under which Kirchhoff's law holds implies that each elementary volume of an atmosphere can be understood to behave like an

enclosure as defined by Kirchhoff. It represents a physical system to which a temperature can be ascribed, so that the local properties of the system are described by Planck's radiation law and Kirchhoff's law. Chandrasekhar (1960) formulated the concept of local thermodynamic equilibrium in the following way:

an atmosphere is said to be in LTE when it is possible to define at each point in the atmosphere a temperature  $T$  such that the coefficients of absorption and emission are related according to the laws of Kirchhoff and Planck.

4 - The integral of the Schwarzschild equation with respect to the depth  $x$ .

Within the domain of validity of Kirchhoff's law, we find that the source function  $\mathcal{J}_\nu$  is identical to the Planck function of enclosure radiation:

$$(5) \quad \mathcal{J}_\nu = \frac{j_0}{\kappa_0} = B_\nu(T)$$

If  $\mu_\nu^2 = 1$ , Schwarzschild's equation assumes the form

$$(6) \quad \frac{\mu}{\rho(x)\kappa_\nu(x,\nu)} \frac{d}{dx} I_\nu(x,\mu,\nu) = I_\nu(x,\mu,\nu) - B_\nu(T)$$

Kourganoff introduces at this point the optical depth

$$(7) \quad \tau_\nu = \tau_\nu(x,\nu) = \int_{-\infty}^x \rho(\xi)\kappa_\nu(\xi,\nu) d\xi$$

We do not follow that course, but rather keep the geometric depth  $x$  as the explicit independent variable. Depth rather than height has been taken for convenience in order to keep the march of the optical and the geometric variable parallel and of the same orientation. The origin of the  $x$ -axis will be put at the altitude of 50 km. The Martian ground sur-

face is found at  $x = 50$  km. The Schwarzschild equation, as given under (6), describes the transfer of radiation of a specified frequency in a given direction  $\mu$ , when the re-emission is defined by the Planck function  $B_\nu$  of the corresponding geometric depth  $x$ .

For a specified frequency, the complete "formal" solution is considered to be:

$$(8) \quad I(x_0, \mu, \nu) = - \exp \left[ \int_{-\infty}^{x_0} \rho(\xi) \kappa_\nu(\xi, \nu) \frac{d\xi}{\mu} \right] \int_c^{x_0} B_\nu(\xi, \nu) \cdot \exp \left[ - \int_{-\infty}^{\xi} \rho(\xi^*) \kappa_\nu(\xi^*, \mu) \frac{d\xi^*}{\mu} \right] \rho(\xi) \kappa_\nu(\xi, \nu) \frac{d\xi}{\mu}$$

In order to determine the constant of integration  $c$ , the distinction between the upward intensity  $I_{\nu+}$ , and downward intensity  $I_{\nu-}$ , is introduced.

Thus we have

$$(9) \quad I_{\nu-}(x_0, \mu, \nu) = \int_0^{x_0} B_\nu(\xi, \nu) \exp \left[ - \int_0^{\xi} \rho(\xi^*) \kappa_\nu(\xi^*, \nu) \frac{d\xi^*}{\mu} + \int_0^{x_0} \rho(\xi^*) \kappa_\nu(\xi^*, \nu) \frac{d\xi^*}{\mu} \right] \rho(\xi) \kappa_\nu(\xi, \nu) \frac{d\xi}{(-\mu)} + \int_c^0 B_\nu(\xi, \nu) \exp \left[ - \int_0^{\xi} \rho(\xi^*) \kappa_\nu(\xi^*, \nu) \frac{d\xi^*}{\mu} + \int_0^{x_0} \rho(\xi^*) \kappa_\nu(\xi^*, \nu) \frac{d\xi^*}{\mu} \right] \rho(\xi) \kappa_\nu(\xi, \nu) \frac{d\xi}{(-\mu)}$$

For convenience, the expression may be rewritten in the form

$$(10) \quad I_{\nu-}(x_0, \mu, \nu) = \int_0^{x_0} B_\nu(\xi, \nu) \frac{\partial \mathcal{T}}{\partial \xi} [(x_0 - \xi), \nu, \mu] d\xi + \int_c^0 B_\nu(\xi, \nu) \frac{\partial \mathcal{T}}{\partial \xi} [(x_0 - \xi), \mu, \nu] d\xi$$

with

$\mathcal{T}$ : transmission function, where

$$(11) \quad \exp \left[ \frac{-f(\xi) + f(x_0)}{\mu} \right] = \mathcal{T}[(x_0 - \xi), \mu, \nu]$$

and

$$(12) \quad \frac{\partial \mathcal{T}}{\partial \xi} [(x_0 - \xi), \nu, \mu] = \exp \left[ \frac{-f(\xi) + f(x_0)}{\mu} \right] \frac{f'(\xi)}{(-\mu)} ; \mu < 0 \text{ for } I_{\nu-}$$

The analytical form of  $I_{\nu-}(x_0, \mu, \nu)$  represents the downward intensity at the level  $x_0$  in the direction  $\mu$  of the frequency  $\nu$ . The first term on the right-hand side of the equation (10) represents contributions of radiation from source functions corresponding to layers above  $x_0$  up to the top of the atmosphere. The second term describes contributions from sources in outer space beyond 50 km. of altitude. This term is definitely negligible for the far IR radiation, whereas the near IR radiation (1 - 5 micron) contained in the solar spectrum must be considered for an evaluation of the (spectral specific) downward intensity, as can be seen in Figure 2 with respect to  $\text{CO}_2$  absorption bands.

Similarly, we find as the analytical expression for the upward intensity

$$(13) \quad I_{\nu+}(x_0, \mu, \nu) = \int_{x_0}^{\infty} B_{\nu}(\xi, \nu) \exp \left[ - \int_{\xi}^{\infty} \rho(\xi^*) \kappa_{\nu}(\xi^*, \nu) \frac{d\xi^*}{\mu} + \int_{\infty}^{x_0} \rho(\xi^*) \kappa_{\nu}(\xi^*, \nu) \frac{d\xi^*}{\mu} \right] \cdot \rho(\xi) \kappa_{\nu}(\xi, \nu) \frac{d\xi}{\mu}$$

This is conveniently rewritten as

$$(14) \quad I_{\nu+}(x_0, \mu, \nu) = \int_{\infty}^{x_0} B_{\nu}(\xi, \nu) \frac{\partial \mathcal{T}[(\xi - x_0), \nu, \mu]}{\partial \xi} d\xi$$

Taking into account that for practical purposes the ground is a black body within the IR range, we may split the right-hand integral and obtain

$$(15) \quad I_{\nu+}(x_0, \mu, \nu) = \int_{\infty}^{x_s} B_{\nu}(\xi, \nu) \frac{\partial \mathcal{T}[(\xi - x_0), \mu, \nu]}{\partial \xi} d\xi + \int_{x_s}^{x_0} B_{\nu}(\xi, \nu) \frac{\partial \mathcal{T}[(\xi - x_0), \mu, \nu]}{\partial \xi} d\xi$$

or better

$$(16) \quad I_{\nu+}(x_0, \mu, \nu) = B_{\nu}(x_s, \nu) \mathcal{T}[(x_s - x_0), \mu, \nu] + \int_{x_s}^{x_0} B_{\nu}(\xi, \nu) \frac{\partial \mathcal{T}[(\xi - x_0), \mu, \nu]}{\partial \xi} d\xi$$



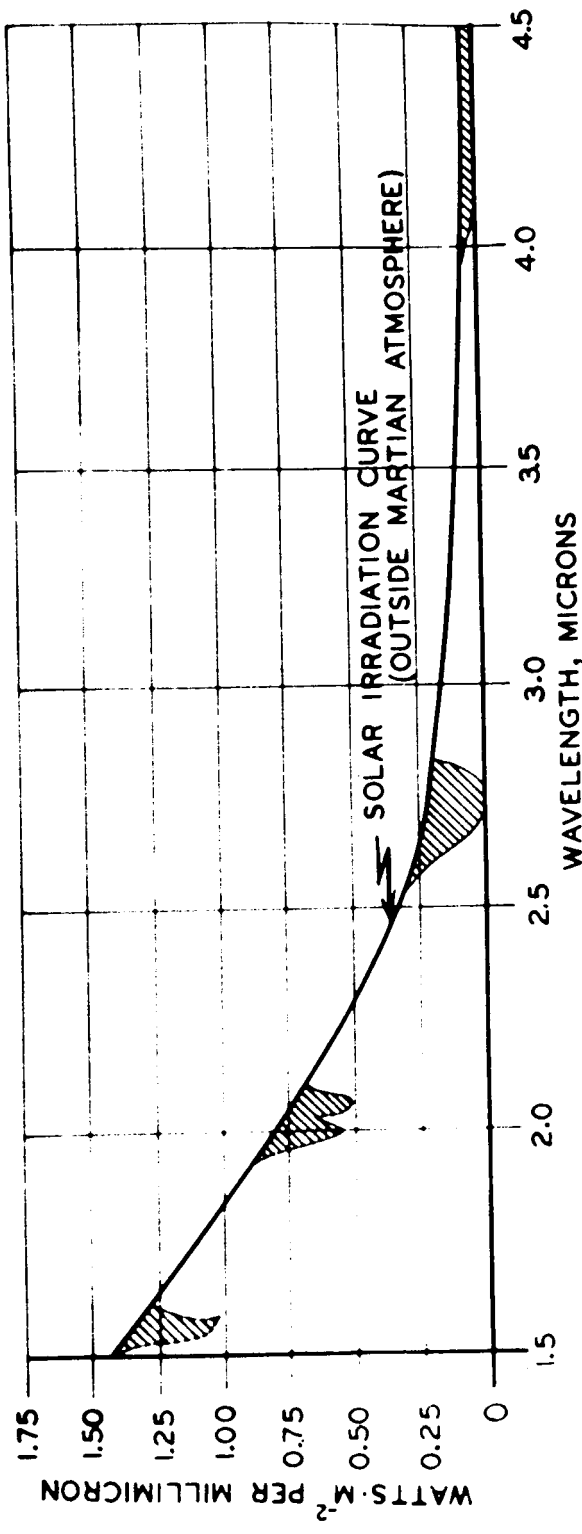


FIG. 2

QUALITATIVE PRESENTATION OF THE CO<sub>2</sub> BAND ABSORPTION  
IN THE LOWER MARTIAN ATMOSPHERE.

It can easily be seen that the part of the radiation which is emitted from the ground surface, is included here by having the integration extended to infinity. The underlying geometry is shown in Figure 3.

5 - The integral of the Schwarzschild equation with respect to the zenith and the azimuth angles.

So far, only "monochromatic beams" were considered. In order to arrive at fluxes, an integration over the hemispheres must be carried out. Conveniently, the spherical coordinates (zenith distance and azimuth) may be taken.

First, the spectral (monochromatic) downward intensity is considered. Elsasser (1960) has shown that under the condition of independence from the azimuth angle (isotropy condition as stipulated earlier), the downward flux may be written as

$$(17) \quad F_{v-} = 2\pi \int_{\pi/2}^{\pi} I_v(\theta) \cos\theta \sin\theta d\theta$$

For the upward flux we find

$$(18) \quad F_{v+} = 2\pi \int_0^{\pi/2} I_v(\theta) \cos\theta \sin\theta d\theta$$

For black body radiation, the spectral flux, under the restrictions indicated before, is related to the Planck function by

$$(19) \quad F_{v,b} = \pi B_v$$

where  $F_{v,b}$  is the spectral net flux for black body radiation. If an atmospheric layer of thickness  $(x_2 - x_1)$  is considered, one finds for a beam

$$(20) \quad I_v = I_{v;0} \mathcal{F}[(x_2 - x_1), \mu, \nu]$$

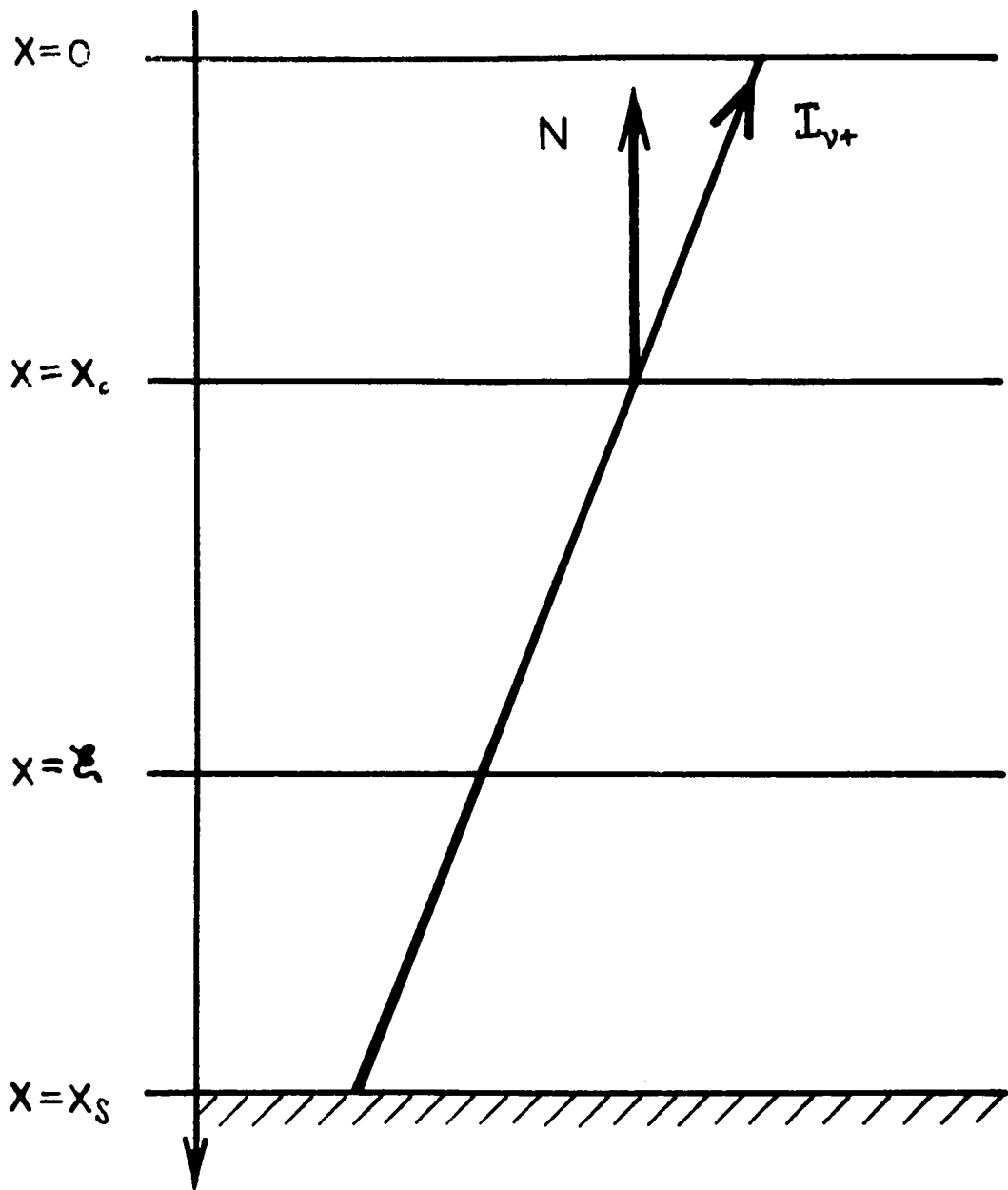


FIG 3

Integrating over the hemisphere, yields

$$(21) \quad F_{v-} = 2(\pi I_{v,o}) \int_{\pi/2}^{\pi} \mathcal{T}[(x_2-x_1), v, \mu] \cos\theta \sin\theta d\theta$$

and

$$(22) \quad F_{v+} = 2(\pi I_{v,o}) \int_0^{\pi/2} \mathcal{T}[(x_2-x_1), \mu, v] \cos\theta \sin\theta d\theta$$

These two equations may be rewritten, using  $F_{v,b} = \pi B_v$ , yielding

$$(23) \quad F_{v-} = F_{v,o}^- \mathcal{T}_F[(x_2-x_1), \mu, v]; \quad \mu < 0$$

with

$$(24) \quad \mathcal{T}_F[(x_2-x_1), v, \mu] = 2 \int_{\pi/2}^{\pi} \mathcal{T}[(x_2-x_1), v, \mu] \cos\theta \sin\theta d\theta$$

as the flux transmissivity;

correspondingly:

$$(25) \quad F_{v+} = F_{v,o}^+ \mathcal{T}_F[(x_2-x_1), v, \mu]; \quad \mu > 0$$

Due to Elsasser (1960), the shape of the  $\mathcal{T}_F$  - function is in all practical cases very similar to that of the beam transmissivity; there is only a slight shift on the x-scale:

$$(26) \quad \mathcal{T}_F[(x_2-x_1), v] = \mathcal{T}[1.60(x_2-x_1), v]$$

The factor 1.6 is to be entered into the implicit function of depth.

6 - The integral with respect to the frequency: total flux.

The integration over the frequency may be carried out in two steps:

(1) expanding from an infinitesimal  $d\nu$  to a finite  $\Delta\nu$  by means of

$$(27) \quad \mathcal{T} = \frac{1}{I_0 \Delta\nu} \int I_\nu d\nu = \frac{1}{\Delta\nu} \int_{\Delta\nu} \exp\left[-\kappa_\nu \int_0 dx\right] d\nu$$

(2) then, the full integration may be performed.

Thus, the integration over the frequency and zenith plus azimuth angles simply calls for the replacement of the intensity  $I_\nu$  by the flux  $F$  and  $\mathcal{T}$  by  $\mathcal{T}_F$ . Doing this, we have finally

$$(28) \quad F_-(x_0) = \pi \int_0^\infty d\nu \int_0^{x_0} B_\nu(\xi, \nu) \frac{\partial \mathcal{T}_F}{\partial \xi}[(x_0 - \xi), \nu] d\xi +$$

+(flux term of depleted solar near-IR rad.)

and

$$(29) \quad F_+(x_0) = \pi \int_0^\infty B_\nu(x_s, \nu) \mathcal{T}_F[(x_s - x_0), \nu] d\nu +$$

$$+ \pi \int_0^\infty d\nu \int_{x_s}^{x_0} B_\nu(\xi, \nu) \frac{\partial \mathcal{T}_F}{\partial \xi}[(\xi - x_0), \nu] d\xi$$

Before we reformulate these two expressions, to have them in a more convenient form for the numerical evaluation, we need to discuss the transmission function further.

7 - The transmission function.

Prabhakara and Hogan (1965) have suggested a "statistical" model transmission function of  $\text{CO}_2$  for which the line intensity is uniform within a given interval of a band, but varies from interval to interval. The ratio of line half-width,  $\alpha$ , to line spacing,  $d$ , is held constant for a particular band.

In its general form the transmission function reads

$$(30) \quad = \exp\left[-\beta x e^{-x} [I_0(x) + I_1(x)]\right]$$

with  $x = \frac{Sw}{2\pi\alpha}$

and  $\beta = \frac{2\pi\alpha}{d}$

S: integrated line intensity                       $\alpha$ : half-width

w: radiational path length                      d: spacing

For the numerical evaluation of  $(I_0 + I_1)$  as a function of  $x$ , see for instance Jahnke & Emde, (1945, who named the Bessel functions of imaginary argument  $J_0(ix)$  and  $-iJ_1(ix)$ ).

Prabhakara & Hogan (1965) provide a table in which the band parameters  $x_0$  and  $\beta_0$  (STP condition) are listed for the near IR absorption of  $CO_2$  as well as 15 micron far IR band. The listing has been based on a thorough investigation of the  $CO_2$  transmission in the region from 1 - 20 micron. The pressure range considered runs from 1 atm to 0.01 atm. (The investigation has been carried out by Stull, Wyatt and Plass, 1963.)

The present author checked very carefully all the formulae offered by Prabhakara & Hogan (1965) as well as those published by Elsasser (1960) and removed minor inconsistencies. The radiational path-length through the absorbing gas has been reduced to standard temperature and pressure (STP) conditions and is given by

$$(31) \quad w = \int_{X_0}^{\xi} \frac{P^*}{P_0} \frac{T_0}{T} \sec\theta d\theta,$$

where  $\sec\theta < 0$  for  $I_{\nu-}$

and  $\sec\theta > 0$  for  $I_{\nu+}$

Since the self-broadening of the CO<sub>2</sub> spectral lines is very efficient, a factor 1.3 to the pressure is appropriate, as indicated by Robinson (1966). The effective pressure is, therefore,

$$P^* = 1.3p$$

instead of p.

By means of the band parameters at STP

$$(32) \quad \frac{S_0 p_0}{2\pi\alpha_0} = C_1$$

and

$$(33) \quad \frac{2\pi\alpha_0}{p_0 d} = C_2$$

and the actual values of the atmospheric pressure and the radiational path-length, the actual band parameters  $x$  and  $\beta$  can easily be computed.

As Prabhakara & Hogan (1965) mention, Hanel and Barko (1964) found that the temperature dependence of the integrated line intensity  $S$  is negligible for the near IR bands up to 5 micron. However, it must be taken into account for the 15 micron band. The present author has made numerical computations for various cases in the far IR range and has come to the conclusion that neglecting this dependence would introduce essential error. The analytical expression for the integrated line intensity as a function of temperature is given by

$$(34) \quad S = S_0 \cdot \exp \left[ \Gamma \left( \frac{1}{T_0} - \frac{1}{T} \right) \right]$$

where

$S$  : the line intensity at temperature  $T$

$S_0$  : the line intensity at temperature  $T_0$  ( $273^\circ\text{K}$ )

$\Gamma$  : coefficient of temperature dependence of the line intensity.

To put more emphasis on this matter, an example is given for the  $825\text{ cm}^{-1}$  spectral line:

$$\text{suppose } T = 150^\circ\text{K}, \quad T_0 = 273^\circ\text{K}, \text{ and } \Gamma = 3 \times 10^3.$$

By applying formula (34), we obtain

$$S = S_0(1.2 \times 10^{-4}).$$

This remarkable result shows how strongly the integrated line intensity depends on the temperature. The result is, however, not surprising if one remembers that in the kinetic gas theory the temperature is interpreted as the average kinetic energy of the molecules, i.e. the very collision activity which is so crucial for the existence of LTE.

The present author has carried out a series of computations to establish consistency between his results and those presented by Prabhakara & Hogan (1965). The agreement is very satisfactory. One of the questions checked was whether or not the strong line approximation is good enough for the weak lines of the near IR absorption bands of  $\text{CO}_2$ . Although there was a difference in the resulting numerical value of the transmission function in its general form and the one in the form for strong lines, the difference is judged to be of minor importance, because the transmission for the weak lines is very large, that is to say, the absorption is very small. Therefore, in the present model of the Martian atmosphere of 100%  $\text{CO}_2$ , with the concentration of the gas gradually but continuously decreasing in the vertical,



the difference between the general form and the strong line approximation of the transmission function is assumed to be immaterial. (First approximation)

Finally, the special form of the transmission function is obtained incorporating all the specifications discussed in this section:

$$(35) \quad \mathcal{T} = \exp - \left[ 0.8 C_2 \left( \frac{T_0}{T} \right)^{1/4} \left( \frac{S_0 P_0}{2\pi \alpha_0} \right)^{1/2} \left[ \exp \Gamma \left( \frac{1}{T_0} - \frac{1}{T} \right) \right]^{1/2} \cdot [w(1.3p)]^{1/2} \right]$$

Taking as the average temperature between 0 and 50 km.  $\bar{T} = 180^\circ\text{K}$ , we find  $(T_0/\bar{T})^{1/4} = (273/180)^{1/4} = 1.11$ . If the total range of the temperature in the Martian troposphere and stratosphere is assumed to run from  $150^\circ\text{K}$  to  $234^\circ\text{K}$ , an inaccuracy of  $\pm 6\%$  is introduced by taking the average temperature instead of the actual level temperature (maximum deviation).

Multiplying through all numerical factors, i.e., 0.8, 1.11,  $(1.3)^{1/2}$ , we obtain 1.01 which is taken as 1.

Thus, we have for the transmission function

$$(36) \quad \mathcal{T} = \exp - \left[ \sqrt{C_1} \cdot C_2 \left[ \exp \Gamma \left( \frac{1}{T_0} - \frac{1}{T} \right) \right]^{1/2} \cdot \sqrt{wp} \right]$$

The expression  $\left( \exp \Gamma \left[ \frac{1}{T_0} - \frac{1}{T} \right] \right)^{1/2}$  assumes the numerical value 1.0 in the case of the near IR bands, as mentioned above. However, for the far IR bands about 15 micron, the numerical value of  $\Gamma$  varies by more than one order of magnitude. A listing of the numerical values of this quantity is included in the table of the band parameters at the end of this report. In order to test the deviations from the value of the transmission function obtained by using the full form of the formula, computations were carried out for which  $\Gamma$  was varied within its listed range. The deviations are considered to be substantial, since the numerical value of the transmission function

may vary by 50%.

In equation (36), the radiational path length  $w$  should be multiplied by the factor 1.6 (as indicated on page 13 of this report), if we go from the beam transmission to the flux transmissivity. Furthermore, equation (31) requires that the path length integral include the pressure which is to be multiplied by 1.3 to account for the intense self-broadening of  $\text{CO}_2$ .

Incorporating these factors and replacing  $(p/p_0) \cdot (T_0/T)$  by  $(\rho/\rho_0)$ , we arrive at the form of the transmission function to be used for the numerical evaluation:

$$(37) \quad \mathcal{T}_F = \exp \left[ C_1 C_2^2 \cdot \left[ \exp \Gamma \left( \frac{1}{T_0} - \frac{1}{T} \right) \right] p(2.1) \left| \int_{x_0}^{\xi} \left( \frac{\rho}{\rho_0} \right) d\xi \right|^{1/2} \right]$$

with  $\rho_0$ : the density of the absorbing gas at STP.

#### 8 - Direct absorption of incoming solar radiation by $\text{CO}_2$ .

An analytical form must be found for that part of the solar radiation which penetrates the Martian atmosphere and is absorbed by carbon dioxide in well-defined near IR bands (Prabhakara & Hogan, 1965, citing Stull, Wyatt and Plass, 1963).

F. Bates presents his temperature curves as mean annual, subsolar meridian-soundings at various latitudes. It is assumed that not only the noon sun but also the solar radiation before and after noon will have an important bearing on the modification of the thermal stratification of the Martian atmosphere at the subsolar meridian. It is proposed, therefore, to consider a sufficiently long time-period rather than a well-determined instant. As a matter of fact, there is no such thing as the direct absorption of near IR solar radiation at an isolated instant followed by an

immediate spread of the generated radiant heat at the same instant.

Therefore, an adequate time interval should be taken within which radiative heating (or cooling) may effectively be produced in an atmospheric scale. It would be plausible to split a 24-hour period into two equal halves, since a mean annual sun is assumed. This assumption implies that the solar orbit be in the equatorial plane.

The equipartition of the diurnal time period, however, does not really take into account the enhanced solar incidence about the noon hour. It is for this reason that the interval

from 9 a.m. to 3 p.m.

is chosen centered at the reference meridian. (The same time interval should be taken for the heating and cooling rates.)

The various latitudes introduce the cos-function for the mean annual sun as Figure 4 shows. The effective cross section of normal incidence for the noon sun can be visualized to be fixed with Mars as the planet rotates about its axis completing a  $(2\pi)$ -radian in 24 hours and 37 minutes. The sin-function of the azimuth angle describes analytically the exposure of the effective cross section to the sun at any instant of Mars' rotation.

In order to obtain the solar incidence totaling over 6 hours (9 a.m. - 3 p.m.) as a first approximation, an average is computed for the sin-function with  $\alpha$  being the azimuth:

$$(38) \quad \frac{2}{\pi} \int_{\pi/4}^{3\pi/4} \sin \alpha d\alpha = \frac{2}{\pi} (-\cos \alpha) \Big|_{\pi/4}^{3\pi/4} = \frac{2}{\pi} \left[ \frac{\sqrt{2}}{2} + \frac{\sqrt{2}}{2} \right]; \quad \frac{2}{\pi} \sin \alpha = \frac{2\sqrt{2}}{\pi}$$

Thus, the solar incidence at the top of the atmosphere and for a latitude of  $\phi$  degrees averaged over the 6-hour interval, may be formulated in the following way:

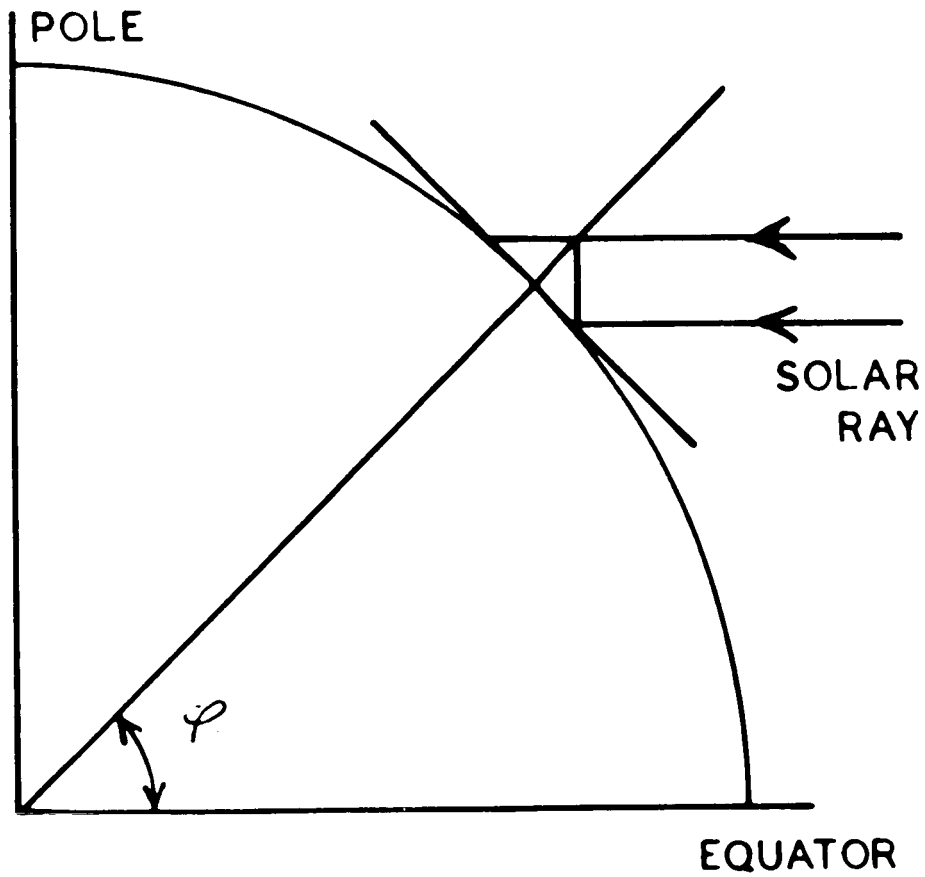


FIG 4

$$(39) \quad \overline{E_o^s(\phi)}_{\text{near IR}} = \frac{2\sqrt{2}}{\pi} \int_{\nu_1}^{\nu_2} E_o^s(\nu) \cos\phi d\nu = \frac{2\sqrt{2}}{\pi} \cos\phi \int_{\nu_1}^{\nu_2} E_o^s(\nu) d\nu$$

where  $E_o^s(\nu)$  is the solar energy within the frequency interval  $(\nu, \nu+d\nu)$  of normal incidence per unit area and per unit time at the top of the atmosphere at the equator.

The near IR solar flux density at the depth  $x_o$  will depend on the spectral transmissivities of the specific absorption bands of  $CO_2$  in the near IR for the atmospheric layer between the top and the depth  $x_o$ . Therefore,  $E_o^s(\nu; \phi)$  is multiplied by the appropriate transmission function, i.e. the beam-transmission function which equals the flux transmissivity whose argument was divided by the factor 1.6, and then integrated over the frequency:

$$(40) \quad \overline{E^s(x_o; \phi)}_{\text{near IR}} = \frac{2\sqrt{2}}{\pi} \cos\phi \int_{\nu_1}^{\nu_2} E_o^s(\nu; \phi=0) \mathcal{T}[(x_o-0), \nu] d\nu$$

This is the formula used in the numerical evaluation.

III. The computational procedure.

1 - The analytical expression of the heating and cooling rates.

As shown in section #2 of the introduction, the heating or cooling rate is given by

$$(41) \quad \frac{\partial T}{\partial t} = - \frac{1}{\rho c_p} \frac{(F_{net}^{(2)} - F_{net}^{(1)})}{\Delta x}$$

with the net flux appropriately defined as

$$(42) \quad F_{net} = (F_{down} - F_{up})$$

in the new coordinate system with  $x$  as depth from 50 km of elevation downward. Formula (41) indicates that the net flux difference has to be considered. Designating by  $F_{up}^{(2)}$  the upward flux at the depth  $x_2$  which is deeper than  $x_1$ , etc., the net flux difference can be formulated by

$$(43) \quad \begin{aligned} \Delta F_{net} &= F_{down}^{(2)} - F_{up}^{(2)} - F_{down}^{(1)} + F_{up}^{(1)} \\ &= F_{down}^{(2)} - F_{down}^{(1)} - [F_{up}^{(2)} - F_{up}^{(1)}] \end{aligned}$$

As can be seen from this expression, the downward as well as the upward fluxes at the depths  $x_2$  and  $x_1$  have to be computed, then their differences formed, in order to obtain the net flux difference between the levels  $x_2$  and  $x_1$ . By applying (41), we would arrive at the numerical value of the heating or cooling rate.

2 - The computational form of the flux expressions.

Looking at the formulae of the downward and upward fluxes, as given by (28) and (29), we realize that double integrals with integrands containing a derivative with respect to the depth  $x$  must be quantitatively evaluated.

Furthermore, the data for the  $\text{CO}_2$  band parameters refer to wave-number  $n$  ( $\text{cm}^{-1}$ ) instead of frequency  $\nu$  ( $\text{sec}^{-1}$ ). The relation between these two quantities is very simple:

$$(44) \quad \nu = cn; \quad d\nu = c \, dn$$

with

$$c = 3 \times 10^{10} \text{ (cm. sec}^{-1}\text{) as the speed of light.}$$

Considering the relation

$$(45) \quad B_\nu(T) \, d\nu = \frac{2h}{c^2} \frac{\nu^3 \, d\nu}{e^{h\nu/KT} - 1} = \frac{2h}{c^2} \frac{c^3 n^3 (c \, dn)}{e^{hcn/KT} - 1} = B_n(T) \, dn$$

we see that we simply replace  $B_\nu \cdot d\nu$  by  $B_n \, dn$  in agreement with Elsasser (1960).

We apply these relationships to (28) and (29) and obtain:

$$(46) \quad F_-(x_0) = \pi \int_0^\infty dn \int_0^{x_0} B_n(\xi, n) \frac{\partial \mathcal{T}[1.6(x_0 - \xi), n]}{\partial \xi} d\xi + \frac{2\sqrt{2} \cos \phi}{\pi} \int_{n=1900 \text{ cm}^{-1}}^{n=7775 \text{ cm}^{-1}} E_0^S(n; \phi=0) \mathcal{T}[(x_0 - 0), n] \, dn$$

for the downward flux, and

$$(47) \quad F_+(x_0) = \pi \int_0^\infty dn \int_{x_s}^{x_0} B_n(\xi, n) \frac{\partial \mathcal{T}[1.60(\xi - x_0), n]}{\partial \xi} d\xi + \pi \int B_n(x_s, n) \mathcal{T}[1.6(x_s - x_0), n] \, dn$$

for the upward flux.

The explicit form of  $B_n$ , the Planck function, is

$$(48) \quad B_n = \frac{(2hc^2)n^3}{e^{hcn/KT} - 1} \quad (\text{ergs.cm}^{-2}.\text{sec}^{-1}.\text{cm.sterad.}^{-1})$$

Additionally, the relationship

$$(49) \quad B_n^F = \pi B_n$$

was used, where

$$(50) \quad B_n^F = \int_0^{2\pi} \int_0^{\pi/2} B_n \cos\theta \sin\theta d\theta d\phi,$$

assuming that  $B_n$  is not a function of the zenith angle  $\theta$  and the azimuth  $\phi$ . This is generally done (see Elsasser, 1960), although it is not exactly true. However, it is certainly sufficient as a first approximation and in the light of all the other assumptions made.

The flux formulae (46) and (47) are rewritten for an easier numerical calculation. First, the wave-number integral is replaced by a sum using the finite-difference method; in the case of the downward flux, we have:

$$(51) \quad F_-(x_0) = \pi \sum_{i=1}^N \Delta n_i \int_0^{x_0} B_n(\xi, n_i) \frac{\partial \mathcal{I}_F[(x_0 - \xi), n_i]}{\partial \xi} d\xi + \\ + \frac{2\sqrt{2}}{\pi} \cos\phi \sum_{k=1}^M E_0^S[n_k; \phi = 0] \mathcal{I}[(x_0 - 0), n_k] \Delta n_k$$

with

N: number of spectral intervals given by the table of the band parameters, excluding the interval ( $1900 \text{ cm}^{-1}$  to  $7775 \text{ cm}^{-1}$ );

M: number of spectral intervals of only the near IR bands excluding the far IR bands (15 micron).



At this point, strong emphasis is put on the fact that the long-wave radiation spectra of the Martian atmosphere with mean temperatures  $T \leq 285^\circ\text{K}$  and maximum intensities due to Wien's displacement law at wave lengths larger than 10 micron (or wave-numbers less than  $1000 \text{ cm}^{-1}$ ) do not contain an energy amount worth mentioning (less than 1% of the total flux density) below 4.5 micron. Therefore, the first right-hand sum strictly refers to the 15 micron bands of  $\text{CO}_2$ , and the second sum refers uniquely to the near IR bands from 1.3 to 4.3 micron. This fact makes the numerical computation much easier.

We have mentioned before, that there are tabulations of the Planck function available. (Jahnke & Emde, 1945: In relation to this table book, a warning must be given. The numerical values are good for plane-polarized radiation; in order to obtain the appropriate unpolarized radiation data, the factor 2 must be applied.)

With respect to formula (51), attention is called to the fact that  $\mathcal{T}_F$  is the flux-transmissivity, see formula (37), whereas in the second right-hand sum is the beam-transmissivity which may be obtained from  $\mathcal{T}_F$  by dividing the argument of this function by the factor 1.6:

$$(52) \quad \mathcal{T}_F\left(\frac{w}{1.6}\right) = \mathcal{T}(w)$$

A tabulation of the solar irradiance is presented in the appendix of this report. The table values must be multiplied by the factor 0.432 to adjust to the condition at the top of the Martian atmosphere.

Additionally, a transformation of the units is needed. The irradiance is given in ( $\text{watts} \cdot \text{cm}^{-2} \cdot \text{micron}^{-1}$ ). The units used are ( $\text{ergs} \cdot \text{sec}^{-1} \cdot \text{cm}^{-2} \cdot \text{cm}^{-1}$ ).

Analogously, we proceed with the upward flux and arrive at

$$(53) \quad F_+(x_o) = \pi \sum_{i=1}^N \Delta n_i \int_{x_s}^{x_o} B_n(\xi, n_i) \frac{\partial \mathcal{J}_F[(\xi - x_o), n]}{\partial \xi} d\xi + \\ + \pi \sum_{i=1}^N \Delta n_i B_n(x_s, n_i) \mathcal{J}_F[(x_s - x_o), n_i]$$

Since the upward flux stems in part from the Martian surface and in part from the atmospheric layers below the reference level  $x_o$  (atmospheric depth), the temperatures involved here are less or equal to  $285^\circ\text{K}$  (atmospheric temperature at the surface as given by F. Bates). The corresponding Planck Function  $B_n(x, n)$  have the characteristics discussed in conjunction with formula (51).

As a next step of adjusting the expressions (46) and (47) for computational purposes, the depth integrals are rewritten as sums applying again the method of finite differences. Thus formula (51) for the downward flux reads

$$(54) \quad F_-(x_o) = \pi \sum_{i=1}^N \Delta n_i \left[ \sum_{m=1}^L B_{n_i}(x_m, n_i) \frac{\Delta \mathcal{J}_F[(x_o - x_m), n_i]}{\Delta x_m} \Delta x_m \right] + \\ + \frac{2\sqrt{2}}{\pi} \cos \phi \sum_{k=1}^M E_o^s(n_k; \phi = 0) \mathcal{J}_F[(x_o - 0), n_k] \Delta n_k$$

As can be seen, we have replaced the differential  $d\xi$  by  $\Delta x_m$ . For a first-approach computation, it seems to be sufficient to assume

$$(55) \quad \Delta x_m = 5 \text{ km.},$$

beginning at the latitude of 50 km which corresponds to  $x = 0$  km of depth:

$$\Delta x_1 = 5 - 0 = 5 \text{ km}$$

$$\Delta x_2 = 10 - 5 = 5 \text{ km}$$

etc.

$$\Delta x_{10} = 50 - 45 = 5 \text{ km}$$

We obtain through this procedure 10 layers each 5 km thick. The troposphere of the midlatitudinal Martian atmosphere consists of 4 of those layers and the stratosphere up to 50 km of altitude is made up of 6 layers. Since the computation of the downward flux  $F_-(x_0)$  should be performed with respect to the reference level  $x_0$ , only those 5 km -- layers will contribute to  $F_-(x_0)$ , which are above  $x_0$ , e.g., if  $x_0 = x_3 = 15$  km, only the layers  $\Delta x_1$ ,  $\Delta x_2$ , and  $\Delta x_3$  will be considered. Thus,  $L$  is a function of the reference level. From here, it follows that

$$(56) \quad \frac{\Delta \mathcal{T}_F[(x_0 - x_m), n_i] \Delta x_m}{\Delta x_m} = \mathcal{T}_F(x_0 - x_j), n_i] - \mathcal{T}_F(x_0 - x_{j-1}), n_i] \text{ with } j = 1, 2, \dots, L$$

means the difference of the two flux transmission functions, see formula (37), where  $x_0$  is the atmospheric depth at which we wish to obtain the downward flux, and  $n_i$  marks the center of the spectral interval chosen.

The geometric detail and the computation method are presented in Figure 5.

The two braces in Figure 5 indicate to which layer each transmission function belongs. However, one must carefully avoid the conclusion, that the difference of the two functions represents the transmission between  $x_2$  and  $x_1$ . That this conclusion cannot be drawn, becomes clear from (37) which presents an exponential function of pressure  $p$ , the temperature  $T$  and the radiational depth.

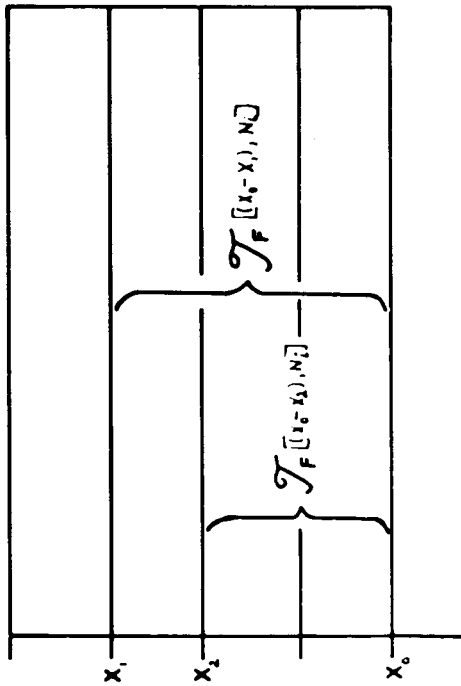


FIG. 5a.  
THE FLUX TRANSMISSIVITY IS THE  
TRANSMISSION FUNCTION OF THE  
LAYER ( $x_0-x_2$ ).

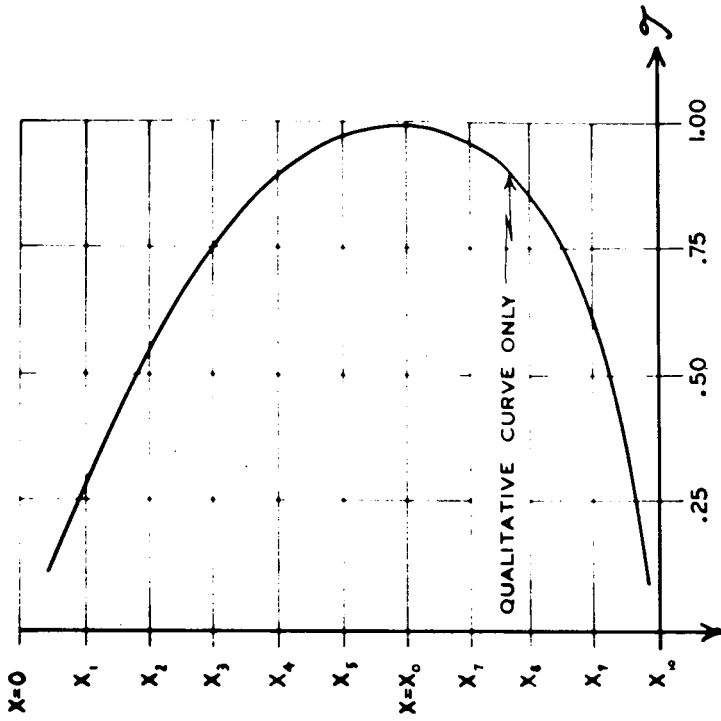


FIG 5b.  
 $J$  HAS A MAXIMUM VALUE OF UNITY AT  
THE REFERENCE LEVEL  $x_0$  AND DECREASES  
IN BOTH DIRECTIONS.

Therefore, for a fixed spectral interval with respect to  $F(x_0)$  the method outlined below should be followed:

first, determine the reference level  $x_0$ ;

second, establish numerically the flux transmission function for all the layers  $(x_0 - x_m)$ , running  $m$  from 1 to  $L$ , where  $x_m = x_0$  is the last level included;

third, form all the differences after formula (56);

fourth, determine the Planck functions corresponding to the depths  $x_m$

(which in effect means a temperature  $T$  ( $^{\circ}\text{K}$ ) from the given sounding);

fifth, multiply those Planck functions  $B_{n_i}(x_m, n_i)$  with the appropriate transmission functions difference;

sixth, add all those products to obtain the sum included in the brackets of the first right-hand term of formula (54);

seventh, multiply this sum with the numerical value of the spectral interval  $\Delta n_i$ .

Now follows the variation of the wave number  $n_i$  (as the central value of the spectral interval given by the table of the band parameters in the Appendix).

For the next spectral interval chosen, one proceeds to the eighth step, i.e., repeating the first to seventh step. Upon completion of the variation of the wave-number  $n_i$ , the frequency sum (first right-hand term of (54)) is numerically established;

ninth, multiply by  $\pi$ , determining thereby the complete first right-hand term.

In a similar fashion, we proceed to numerically evaluate the second right-hand term which is easier since only the frequency sum has to be determined. The numerical values of the solar irradiance  $E_0^S(n_k; \phi=0)$  are given in the Appendix.

Turning to the upward flux in (53), we again express the depth integral by means of a sum:

$$(57) \quad F_+(x_0) = \pi \sum_{i=1}^N \Delta n_i \left[ \sum_{m=1}^L B_{n_i}(x_m, n_i) \mathcal{T}_F[(x_m - x_0), n_i] + \sum_{i=1}^N \Delta n_i B_{n_i}(x_s, n_i) \mathcal{T}_F[(x_s - x_0), n_i] \right]$$

The procedure is analogous to the nine steps discussed above. The second right-hand term of (57) which is the radiation coming from the ground and partially depleted by the interfering layer ( $x_s - x_0$ ), represents only the frequency or better the wave-number sum. Therefore, it is easier to evaluate. Once more, it is emphasized that the flux transmission function given by expression (37) is an exponential function for which the functional argument is a square root; among other factors within that argument, we find the atmospheric pressure and the radiational depth in form of an integral. This integral is numerically calculated by replacing it with a finite-difference sum taking as the depth increment  $dx$  a thickness of 5 km. Since the layer is eventually 50 km of depth, the pressure  $p$  is to be taken as the mean pressure of the layer. This approach to the flux transmission function and its numerical evaluation may be extended to the transmissivities in the other terms of the upward and the downward fluxes.

### 3 - The computation of the heating or cooling rate.

Once we have determined the upward and the downward fluxes not only for one specific reference level  $x_0$ , but for all possible reference levels, i.e. for  $x_0$  being equal to 0, 5, 10, 15, 20, 25, 30, 35, 40, 45, and 50 km of depth (11 depth levels), then we proceed to numerically calculate the net flux difference as indicated in formula (43).

It is recommended to have a close look at Figure 6 to keep procedures in order.

Upon completion of the numerical evaluation of the net flux differences, these must be divided by the negative product of the density times the specific heat at constant pressure of  $\text{CO}_2$  times the depth increment of 5 km. This will immediately present the numerical figure of the rate of heating or cooling, after the appropriate adjustment of the time increment has been made. Since the tabulations of the Planck function as well as those of the solar irradiance are commonly given per second, we would receive values of the heating or cooling rates in degrees Kelvin per second. However, since a six-hour average was applied for the solar radiation incident at the top of the Martian atmosphere, a heating rate in  $^{\circ}\text{K}\text{-sec}^{-1}$  averaged over six-hours is obtained. See our discussion of the matter on page 20 of this report.

It is evident that those values of the heating or cooling rates refer to the centers of the 5 km - layers, in other words, if the net flux difference had been computed between 10 and 15 km of depth as an example, the rate would refer to 12.5 km.

Thus, the complete computation yields 10 data points for the heating or cooling rates over a depth of 50 km. A profile curve of the six-hourly heating or cooling may be drawn.

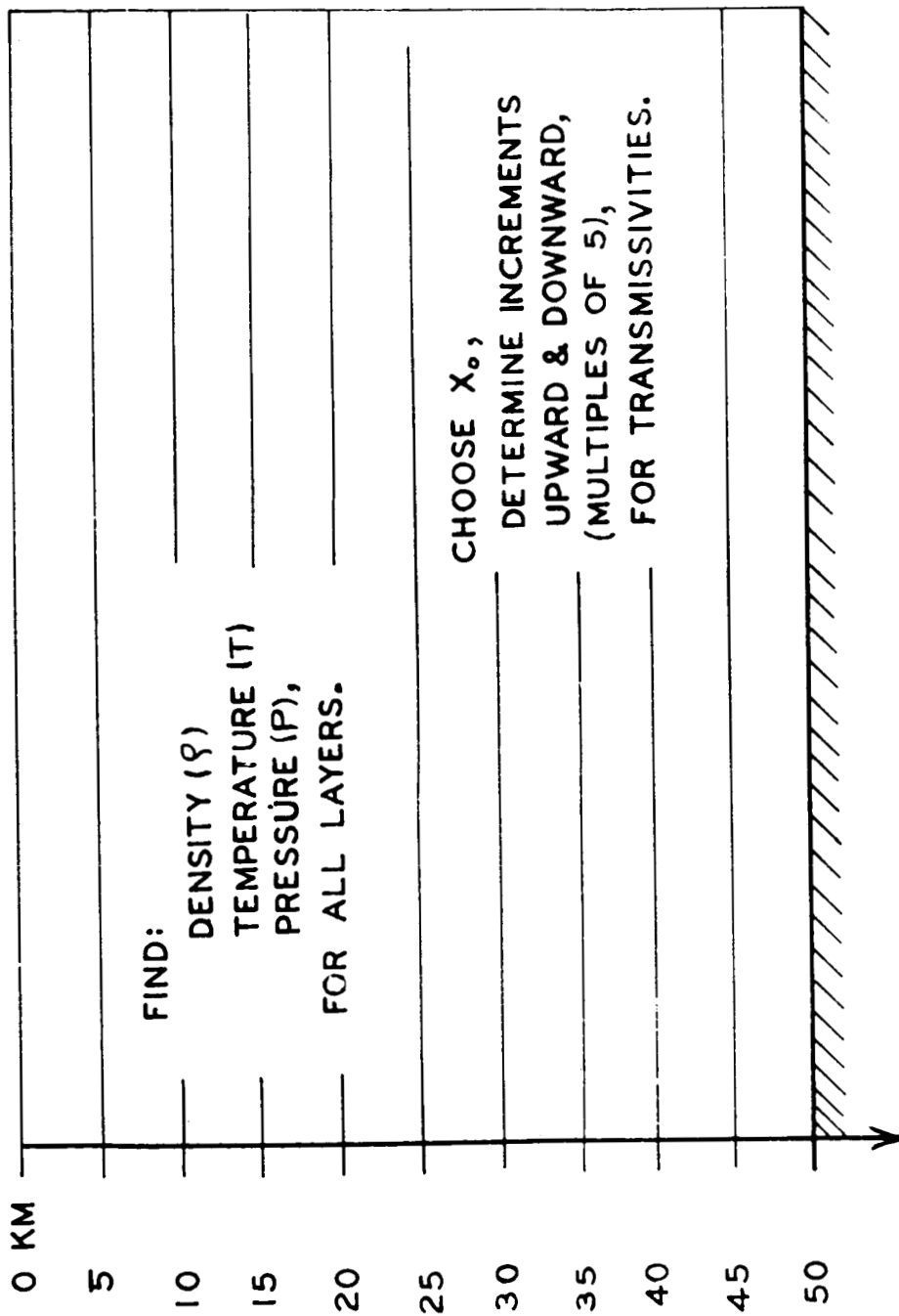


FIG. 6  
 OL .AY OF COMPUTATIONAL SCHEME.



## Appendix I.

TABLE OF THE CO<sub>2</sub> BAND PARAMETERS

| bands<br>(micron) | k  | interval<br>(cm <sup>-1</sup> ) | C <sub>1</sub><br>(atm.cm <sup>-1</sup> ) | C <sub>2</sub><br>(atm <sup>-1</sup> ) |
|-------------------|----|---------------------------------|---|--|
| 1.3               | 1  | 7775-7725                       | 5.0 x 10 <sup>-4</sup>                    | 0.30                                   |
|                   | 2  | 7725-7675                       | 1.2 x 10 <sup>-4</sup>                    | 0.30                                   |
|                   | 3  | 7675-7625                       | 1.5 x 10 <sup>-5</sup>                    | 0.30                                   |
|                   | 4  | 7625-7575                       | 2.0 x 10 <sup>-3</sup>                    | 0.30                                   |
|                   | 5  | 7575-7525                       | 1.3 x 10 <sup>-4</sup>                    | 0.30                                   |
|                   | 6  | 7525-7475                       | 2.0 x 10 <sup>-4</sup>                    | 0.30                                   |
|                   | 7  | 7475-7425                       | 7.2 x 10 <sup>-4</sup>                    | 0.30                                   |
|                   | 8  | 7425-7375                       | 1.8 x 10 <sup>-5</sup>                    | 0.30                                   |
| 1.4               | 9  | 7025-6975                       | 9.2 x 10 <sup>-4</sup>                    | 0.30                                   |
|                   | 10 | 6975-6925                       | 2.0 x 10 <sup>-3</sup>                    | 0.30                                   |
|                   | 11 | 6925-6875                       | 1.2 x 10 <sup>-3</sup>                    | 0.30                                   |
| 1.6               | 12 | 6575-6525                       | 2.9 x 10 <sup>-6</sup>                    | 0.30                                   |
|                   | 13 | 6525-6475                       | 9.0 x 10 <sup>-5</sup>                    | 0.30                                   |
|                   | 14 | 6475-6425                       | 2.9 x 10 <sup>-6</sup>                    | 0.30                                   |
|                   | 15 | 6425-6375                       | 6.4 x 10 <sup>-6</sup>                    | 0.30                                   |
|                   | 16 | 6375-6325                       | 7.0 x 10 <sup>-4</sup>                    | 0.30                                   |
|                   | 17 | 6325-6275                       | 2.5 x 10 <sup>-5</sup>                    | 0.30                                   |
|                   | 18 | 6275-6225                       | 3.5 x 10 <sup>-4</sup>                    | 0.30                                   |
|                   | 19 | 6225-6175                       | 2.3 x 10 <sup>-4</sup>                    | 0.30                                   |
|                   | 20 | 6175-6125                       | 1.0 x 10 <sup>-5</sup>                    | 0.30                                   |
|                   | 21 | 6125-6075                       | 5.5 x 10 <sup>-5</sup>                    | 0.30                                   |

Appendix I.

TABLE OF THE CO<sub>2</sub> BAND PARAMETERS

| bands<br>(micron) | k  | interval<br>(cm <sup>-1</sup> ) | C <sub>1</sub><br>(atm.cm <sup>-1</sup> ) | C <sub>2</sub><br>(atm <sup>-1</sup> ) |
|-------------------|----|---------------------------------|---|--|
|                   | 22 | 6075-6025                       | 1.0 x 10 <sup>-5</sup>                    | 0.30                                   |
| 2.0               | 23 | 5200-5150                       | 3.9 x 10 <sup>-6</sup>                    | 0.33                                   |
|                   | 24 | 5150-5100                       | 3.5 x 10 <sup>-2</sup>                    | 0.33                                   |
|                   | 25 | 5100-5050                       | 3.0 x 10 <sup>-2</sup>                    | 0.33                                   |
|                   | 26 | 5050-5000                       | 7.5 x 10 <sup>-3</sup>                    | 0.33                                   |
|                   | 27 | 5000-4950                       | 5.3 x 10 <sup>-1</sup>                    | 0.33                                   |
|                   | 28 | 4950-4900                       | 2.0 x 10 <sup>-2</sup>                    | 0.33                                   |
|                   | 29 | 4900-4850                       | 1.0 x 10 <sup>-1</sup>                    | 0.33                                   |
|                   | 30 | 4850-4800                       | 6.0 x 10 <sup>-2</sup>                    | 0.33                                   |
|                   | 31 | 4800-4750                       | 1.3 x 10 <sup>-3</sup>                    | 0.33                                   |
|                   | 32 | 4750-4700                       | 3.0 x 10 <sup>-4</sup>                    | 0.33                                   |
| 2.7               | 33 | 3850-3800                       | 1.0 x 10 <sup>-4</sup>                    | 0.36                                   |
|                   | 34 | 3800-3750                       | 2.0 x 10 <sup>-3</sup>                    | 0.36                                   |
|                   | 35 | 3750-3700                       | 2.7 x 10 <sup>1</sup>                     | 0.36                                   |
|                   | 36 | 3700-3650                       | 5.0 x 10 <sup>0</sup>                     | 0.36                                   |
|                   | 37 | 3650-3600                       | 1.7 x 10 <sup>1</sup>                     | 0.36                                   |
|                   | 38 | 3600-3550                       | 6.0 x 10 <sup>0</sup>                     | 0.36                                   |
|                   | 39 | 3550-3500                       | 2.1 x 10 <sup>-1</sup>                    | 0.36                                   |
|                   | 40 | 3500-3450                       | 5.0 x 10 <sup>-3</sup>                    | 0.36                                   |
|                   | 41 | 3450-3425                       | 2.0 x 10 <sup>-5</sup>                    | 0.36                                   |

## Appendix I.

TABLE OF THE CO<sub>2</sub> BAND PARAMETERS

| bands<br>(micron)                         | k  | interval<br>(cm <sup>-1</sup> ) | C <sub>1</sub><br>(atm.cm <sup>-1</sup> ) | C <sub>2</sub><br>(atm <sup>-1</sup> ) | Gamma<br>(°K)         |
|---|----|---------------------------------|---|--|-----------------------|
| 4.3                                       | 42 | 2470-2450                       | 2.2 x 10 <sup>-5</sup>                    | 0.86                                   |                       |
|   | 43 | 2450-2430                       | 2.0 x 10 <sup>-5</sup>                    | 0.86                                   |                       |
|   | 44 | 2430-2410                       | 5.0 x 10 <sup>-4</sup>                    | 0.86                                   |                       |
|   | 45 | 2410-2390                       | 3.2 x 10 <sup>-3</sup>                    | 0.86                                   |                       |
|   | 46 | 2390-2370                       | 1.6 x 10 <sup>0</sup>                     | 0.86                                   |                       |
|   | 47 | 2370-2350                       | 7.0 x 10 <sup>1</sup>                     | 0.86                                   |                       |
|   | 48 | 2350-2300                       | 2.0 x 10 <sup>1</sup>                     | 0.86                                   |                       |
|   | 49 | 2300-2250                       | 7.0 x 10 <sup>-1</sup>                    | 0.86                                   |                       |
|   | 50 | 2250-2200                       | 6.0 x 10 <sup>-3</sup>                    | 0.86                                   |                       |
|   | 51 | 2200-2150                       | 6.6 x 10 <sup>-5</sup>                    | 0.86                                   |                       |
|   | 52 | 2150-2100                       | 1.0 x 10 <sup>-3</sup>                    | 0.35                                   |                       |
|   | 53 | 2100-2050                       | 2.0 x 10 <sup>-2</sup>                    | 0.35                                   |                       |
|   | 54 | 2050-2000                       | 1.0 x 10 <sup>-3</sup>                    | 0.35                                   |                       |
|   | 55 | 2000-1950                       | 5.0 x 10 <sup>-5</sup>                    | 0.35                                   |                       |
|   | 56 | 1950-1900                       | 2.0 x 10 <sup>-3</sup>                    | 0.35                                   |                       |
| far IR absorption band of CO <sub>2</sub> |    |                                 |   |  |                       |
|   | i  |                                 |   |  |                       |
| 15  | 1  | 850-800                         | 2,5 x 10 <sup>-5</sup>                    | 0.24                                   | 3.0 x 10 <sup>3</sup> |
|   | 2  | 800-750                         | 2.0 x 10 <sup>-3</sup>                    | 0.24                                   | 2.0 x 10 <sup>3</sup> |
|   | 3  | 750-700                         | 5.0 x 10 <sup>-1</sup>                    | 0.24                                   | 1.3 x 10 <sup>3</sup> |

far IR absorption band of CO<sub>2</sub> cont.

|   |         |                      |      |                   |
|---|---------|----------------------|------|-------------------|
| 4 | 700-650 | $4.5 \times 10^1$    | 0.24 | $4.0 \times 10^2$ |
| 5 | 650-600 | $2.5 \times 10^0$    | 0.24 | $1.0 \times 10^3$ |
| 6 | 600-550 | $1.0 \times 10^{-2}$ | 0.24 | $2.0 \times 10^3$ |

Appendix II.

SOLAR SPECTRAL IRRADIANCE DATA  
(after Robinson, N.; data from J.S. Johnson)

The mean zero air mass spectral irradiance  $H_\lambda$  is in ( $\text{watts.cm}^{-2}.\text{micron}^{-1}$ );

| wave-number<br>( $\text{cm}^{-1}$ ) | wave-length<br>(micron) | $H_\lambda$ |
|-------------------------------------|-------------------------|-------------|
| k                                   |                         |             |
| 1                                   | 7750                    | 0.0415      |
| 2                                   | 7700                    | .0406       |
| 3                                   | 7650                    | .0398       |
| 4                                   | 7600                    | .0390       |
| 5                                   | 7550                    | .0386       |
| 6                                   | 7500                    | .0378       |
| 7                                   | 7450                    | .0373       |
| 8                                   | 7400                    | .0367       |
| 9                                   | 7000                    | .0310       |
| 10                                  | 6950                    | .0304       |
| 11                                  | 6900                    | .0297       |
| 12                                  | 6550                    | .0253       |
| 13                                  | 6500                    | .0248       |
| 14                                  | 6450                    | .0243       |
| 15                                  | 6400                    | .0238       |
| 16                                  | 6350                    | .0232       |
| 17                                  | 6300                    | .0226       |
| 18                                  | 6250                    | .0220       |
| 19                                  | 6200                    | .0216       |
| 20                                  | 6150                    | .0209       |
| 21                                  | 6100                    | .0204       |
| 22                                  | 6050                    | .0199       |
| 23                                  | 5175                    | .01214      |
| 24                                  | 5125                    | .01177      |
| 25                                  | 5075                    | .01139      |
| 26                                  | 5025                    | .01100      |
| 27                                  | 4975                    | .01063      |
| 28                                  | 4925                    | .01031      |
| 29                                  | 4875                    | .01000      |
| 30                                  | 4825                    | .00965      |

## Appendix cont.

| wave-number<br>( $\text{cm}^{-1}$ ) | wave-length<br>(micron) | $H_{\lambda}$ |
|-------------------------------------|-------------------------|---------------|
| k                                   |                         |               |
| 31 4775                             | 2.09                    | .00947        |
| 32 4725                             | 2.12                    | .00887        |
| 33 3825                             | 2.62                    | .00434        |
| 34 3775                             | 2.65                    | .00417        |
| 45 3725                             | 2.69                    |               |
| 36 3675                             | 2.72                    | .00380        |
| 37 3625                             | 2.76                    | .00362        |
| 38 3575                             | 2.80                    | .00343        |
| 39 3525                             | 2.84                    | .00327        |
| 40 3475                             | 2.875                   | .00313        |
| 41 3438                             | 2.91                    | .00300        |
| 42 2460                             | 4.06                    | .00090        |
| 43 2440                             | 4.1                     | .00087        |
| 44 2420                             | 4.14                    | .00084        |
| 45 2400                             | 4.17                    | .00082        |
| 46 2380                             | 4.20                    | .00080        |
| 47 2360                             | 4.24                    | .00077        |
| 48 2325                             | 4.3                     | .00073        |
| 49 2275                             | 4.4                     | .00067        |
| 50 2225                             | 4.5                     | .00061        |
| 51 2175                             | 4.6                     | .00056        |
| 52 2125                             | 4.7                     | .00051        |
| 53 2075                             | 4.8                     | .00048        |
| 54 2025                             | 4.95                    | .00043        |
| 55 1975                             | 5.05                    | .00041        |
| 56 1925                             | 5.2                     | .00037        |

## BIBLIOGRAPHY

- Busbridge, I.W., 1960: The mathematics of radiative transfer, Cambridge At The University Press.
- Chandrasekhar, S., 1960: Radiative Transfer, Dover Publ.; New York.
- Elsasser, W.M., 1960: Atmospheric radiation tables, American Met. Soc., monograph #23, Boston.
- Finkelburg, W., 1964: Structure of matter, Springer Verlag, Berlin.
- Goody, R.M., 1964: Atmospheric radiation I, theoretical basis, At The Clarendon Press, Oxford.
- Jahnke E. & Emde, F., 1945: Tables of functions with formulae and curves, Dover Publ., New York.
- Kondrat'yev, K. Ya., 1965: Radiative heat exchange in the atmosphere, Pergamon Press, Oxford.
- Kourganoff, V.m 1963: Basic methods in transfer problems, Dover Publ., New York.
- Moeller, F., 1957: Strahlung in der unteren Atmosphaere; Handbuch der Physik, vol. XLVIII, Geophysik II, ed. by Fluegge, S.; Springer Verlag, Berlin.
- Moeller, F. & Manabe, S., 1961: Ueber das Strahlungsgleichgewicht der Atmosphaere, Zeitschrift fuer Meteorologie 15, 1.
- Manabe S. & Moeller, F., 1961: On the radiative equilibrium and heat balance of the atmosphere, Monthly Weather Review 89, 12; Washington.
- Pivovonsky, M. & Nagel, M.R., 1961: Tables of black body radiation functions, Macmillan, New York.
- Prabhakara, C. & Hogan, J.S., 1965: Ozone and Carbon dioxide heating in the Martian atmosphere, J. Atm. Sc. 22, 2.
- Robinson, N. (ed.), 1966: Solar radiation, Elsevier Publ. Co., Amsterdam.
- Schwarzschild, K., 1906: Ueber das Gleichgewicht der Sonnenatmosphaere, Goettinger Nachr. 41.
- Sobolev, V.V., 1963: A treatise on radiative transfer, Van Nostrand Co., New York.
- Stull, V.R., P.J. Wyatt and G.N. Plass, 1963: The infrared absorption of carbon dioxide. Infrared transmission studies III, Rpt. Contract SSD-TDR-62-127, Space Systems Division, Air Force Systems Command, Los Angeles, Calif.